Received: 10 October 2023 | Revised: 13 December 2023 | Accepted: 26 December 2023

DOI: 10.1111/cts.13722

ARTICLE

Population pharmacokinetics, enzyme occupancy, and pharmacodynamic modeling of soticlestat in patients with developmental and epileptic encephalopathies

Wei Yin[1] | **Axel Facius**[2] | **Mahnaz Asgharnejad**[1] | **Gëzim Lahu**[2] | **Majid Vakilynejad**[1,*]

[1]Takeda Pharmaceutical Company Ltd., Cambridge, Massachusetts, USA

[2]thinkQ[2] AG, Baar, Switzerland

Correspondence
Wei Yin, Takeda Development Center Americas, Inc., 35 Landsdowne St, Cambridge, MA 02139, USA.
Email: wei.yin@takeda.com

Abstract

Soticlestat (TAK-935) is a first-in-class, selective inhibitor of cholesterol 24-hydroxylase (CH24H) under phase III development for the treatment of the developmental and epileptic encephalopathies (DEEs), Dravet syndrome (DS), and Lennox–Gastaut syndrome (LGS). A previous model characterized the pharmacokinetics (PKs), CH24H enzyme occupancy (EO), and pharmacodynamics (PDs) of soticlestat in healthy volunteers. The present study extended this original model for patients with DEEs and investigated sources of variability. Model-based simulations were carried out to optimize dosing strategies for use in clinical trials. Data from eight phase I and II trials of healthy volunteers or patients with DEEs receiving oral soticlestat 15–1350 mg were included, encompassing 218 individuals for population PK (PopPK) analyses and 306 individuals for PK/PD analyses. Dosing strategies were identified through model-based simulations. The final mixed-effect PopPK/EO/PD model consisted of a two-compartment PK model and an effect-site compartment in the PK/EO model; soticlestat concentrations at the effect site were linked to 24*S*-hydroxycholesterol plasma concentrations using a semimechanistic inhibitory indirect response model. Covariates were included to account for sources of variability. Pediatric dosing strategies were developed for four body weight bands (10 to <15, 15 to <30, 30 to <45, and 45–100 kg) to account for covariate effects by body weight. The final PopPK and PK/EO/PD models accurately described PK, EO, and PD profiles of soticlestat in healthy volunteers and patients with DEEs. Covariate analyses and model-based simulations facilitated optimization of phase III trial dosing strategies for patients with DS or LGS.

Wei Yin and Axel Facius contributed equally to this work and should be considered co-first authors.

*Affiliation at the time the study was conducted.

Study Highlights

WHAT IS THE CURRENT KNOWLEDGE ON THE TOPIC?

Soticlestat (TAK-935), a selective inhibitor of cholesterol 24-hydroxylase, is in phase III development for the treatment of Dravet syndrome (DS) and Lennox–Gastaut syndrome (LGS). A model was previously developed to characterize the pharmacokinetic (PK) and pharmacodynamic (PD) profiles of soticlestat in healthy volunteers.

WHAT QUESTION DID THIS STUDY ADDRESS?

What are the PK and PD profiles of soticlestat in pediatric and adult patients with developmental and epileptic encephalopathies (DEEs), which covariates affect the PK and PD profiles of soticlestat, and which dosing strategies are suggested for phase III clinical trials in pediatric patients with DS or LGS?

WHAT DOES THIS STUDY ADD TO OUR KNOWLEDGE?

The observed data from healthy adults, and pediatric and adult patients with DEEs were adequately described by a population mixed-effects model in terms of PK and PD profiles. Bodyweight, ethnic background (for people of Chinese or Japanese descent), and patient status affected the PK profile of soticlestat. Weight-based dosing strategies were developed from model-based simulations for use in phase III clinical trials in children and adolescents with DS and LGS with a body weight of less than 60 kg.

HOW MIGHT THIS CHANGE CLINICAL PHARMACOLOGY OR TRANSLATIONAL SCIENCE?

These findings illustrate the value of model-based simulations to select dosing strategies for clinical trials and to understand the impact of covariates on exposure and PD profiles.

INTRODUCTION

Developmental and epileptic encephalopathies (DEEs) are a diverse group of severe epilepsies that include Dravet syndrome (DS) and Lennox–Gastaut syndrome (LGS). DEEs typically begin in childhood and are associated with seizures and developmental delay or regression. Treatments that specifically target pediatric-onset epilepsies are rare and DEEs are often resistant to conventional antiseizure medications (ASMs).[1–3]

Soticlestat (TAK-935) is a first-in-class, selective inhibitor of cholesterol 24-hydroxylase (CH24H; also known as cytochrome P450 [CYP] 46A1).[3,4] CH24H is the primary enzyme responsible for the catabolism of cholesterol to 24*S*-hydroxycholesterol (24HC) in the brain.[4–6] 24HC is a positive allosteric modulator of the N-methyl-D-aspartate receptor that can contribute to neuronal hyperexcitability.[7,8] As such, a reduction in levels of 24HC in the brain could lead to decreased neuronal hyperexcitability and reduced seizure susceptibility. Phase III studies investigating the efficacy, safety, and tolerability of adjunctive soticlestat in pediatric and adult participants with DS and LGS are ongoing (ClinicalTrials.gov: NCT04940624, NCT04938427, and NCT05163314).

Dosing strategies for two phase II trials of soticlestat treatment were developed using model-informed drug development (MIDD), as described in a previous publication.[9] Briefly, a model was developed to describe the pharmacokinetic (PK), enzyme occupancy (EO), and pharmacodynamic (PD) profiles of soticlestat based on data from four phase I studies characterizing soticlestat treatment in healthy volunteers.[9] Model-based simulations indicated that soticlestat 100–300 mg twice-daily (b.i.d.) may be an optimal adult dosing regimen, with weight-adjusted pediatric dosing strategies identified for evaluation in phase II clinical trials.

The suggested model-based dosing strategies were applied in a phase Ib/IIa clinical trial in adults with DEEs[3] and a phase II clinical trial in children with DS or LGS (ELEKTRA, NCT03650452).[10] In the phase Ib/IIa study, soticlestat dosages up to 300 mg b.i.d. were associated with primarily mild treatment-emergent adverse events. Exploratory efficacy evaluation suggested that soticlestat treatment led to a reduction in seizure frequency in the open-label study period.[3] In ELEKTRA, soticlestat treatment resulted in statistically significant and clinically meaningful reductions from baseline in median seizure frequency for the combined patient population, and in

convulsive seizure frequency for the DS cohort. Drop seizure frequency was reduced in children with LGS; however, this change was not statistically significant. Safety findings were consistent with previous studies.[10]

In the present analyses, the PK/EO/PD model developed for healthy volunteers was extended to patients with DEEs. The aims were to: characterize the PKs of soticlestat in pediatric and adult patients with DEEs; characterize the PK/PD relationship between soticlestat concentrations and plasma 24HC concentrations in this population; and evaluate sources of variability, including covariates, that affect the PK and PD profiles of soticlestat. Additionally, model-based simulations were carried out with the aim of developing optimized weight-based dosing strategies for use in phase III clinical studies of soticlestat in children with DS or LGS.

METHODS

Study population and data collection

The present analyses used data from eight clinical trials (Table S1), including the four phase I studies in healthy adult volunteers that were used to develop the original PK/EO/PD model.[9] The additional four trials were the phase Ib/IIa clinical trial in adults with DEEs[3] and the phase II ELEKTRA study[10] discussed above, a phase I study in healthy Japanese adult volunteers (NCT04461483),[11] and a phase II study in children with 15q duplication syndrome or cyclin-dependent kinase-like 5 (CDKL5) deficiency disorder (ARCADE, NCT03694275).[12] Soticlestat was administered as either an oral solution or as tablets with varying dosages across the studies.

Additional details and bioanalytical methods for plasma soticlestat and 24HC levels are provided in the supplementary information. Sampling schedules are summarized in Table S1.

All studies were conducted in accordance with International Council for Harmonization Good Clinical Practice guidelines, applicable local regulations, and the ethical principles that have their origin in the Declaration of Helsinki. All participants gave written informed consent prior to participation in the studies.

Modeling strategy

The modeling process is presented in Figure 1. The original population PK (PopPK) and PK/EO/PD models fit the observed data well from the four healthy volunteer studies.[9] In the present analysis, model refinements were considered to improve the fit to the expanded data set of all eight clinical trials, including data from healthy volunteers and patients with DEEs. Considerations for model refinements encompassed updates to the structural and error-term modeling; for example, optimization of the Omega matrix (restricted to a diagonal structure) for the PopPK model, testing the addition or removal of compartments, adjusting for nonlinear kinetics, and testing various residual error models and transformations of the between-subject variability (BSV) models. Interindividual variability was added for the model parameters with random effects and covariate screening was carried out to identify factors that impact on model parameters.

Data

All data except for the high-fat meal arm of the bioavailability study (TAK-935-1005) and the open-label extension of ELEKTRA (i.e., the ongoing ENDYMION 1 study NCT03635073) were included in the PopPK model refinement. Overall, data were available from 218 participants, consisting of 3288 soticlestat PK observations and 8732 dosing events.

Seven clinical trials were included in the PK/EO/PD model refinement. Data from the bioavailability study were excluded because 24HC concentrations were not collected. Data from the ongoing open-label extension of ELEKTRA were also excluded. Overall, data were available from 306 participants, consisting of 2621 plasma 24HC concentrations and 8703 dosing events.

Apart from the exceptions listed above, no data were excluded. Missing data were not imputed except for the imputation of missing alpha-1-acid glycoprotein (AGP) as the median of the observed values (20 mg/dL).

Software

The modeling was conducted using NONMEM version 7.4.1 (ICON Development Solutions). Data processing and graph development were carried out with R version 3.2 or higher (R Core Team).

Model assessment and comparison

Model selection was based on evaluation of several initial structural models that were assessed against prespecified criteria, including those for goodness-of-fit (GOF). Models were assessed based on individual and population parameter estimates and their precision (relative standard error), numerical convergence properties, biological plausibility, diagnostic and GOF plots, shrinkage of BSV and residual

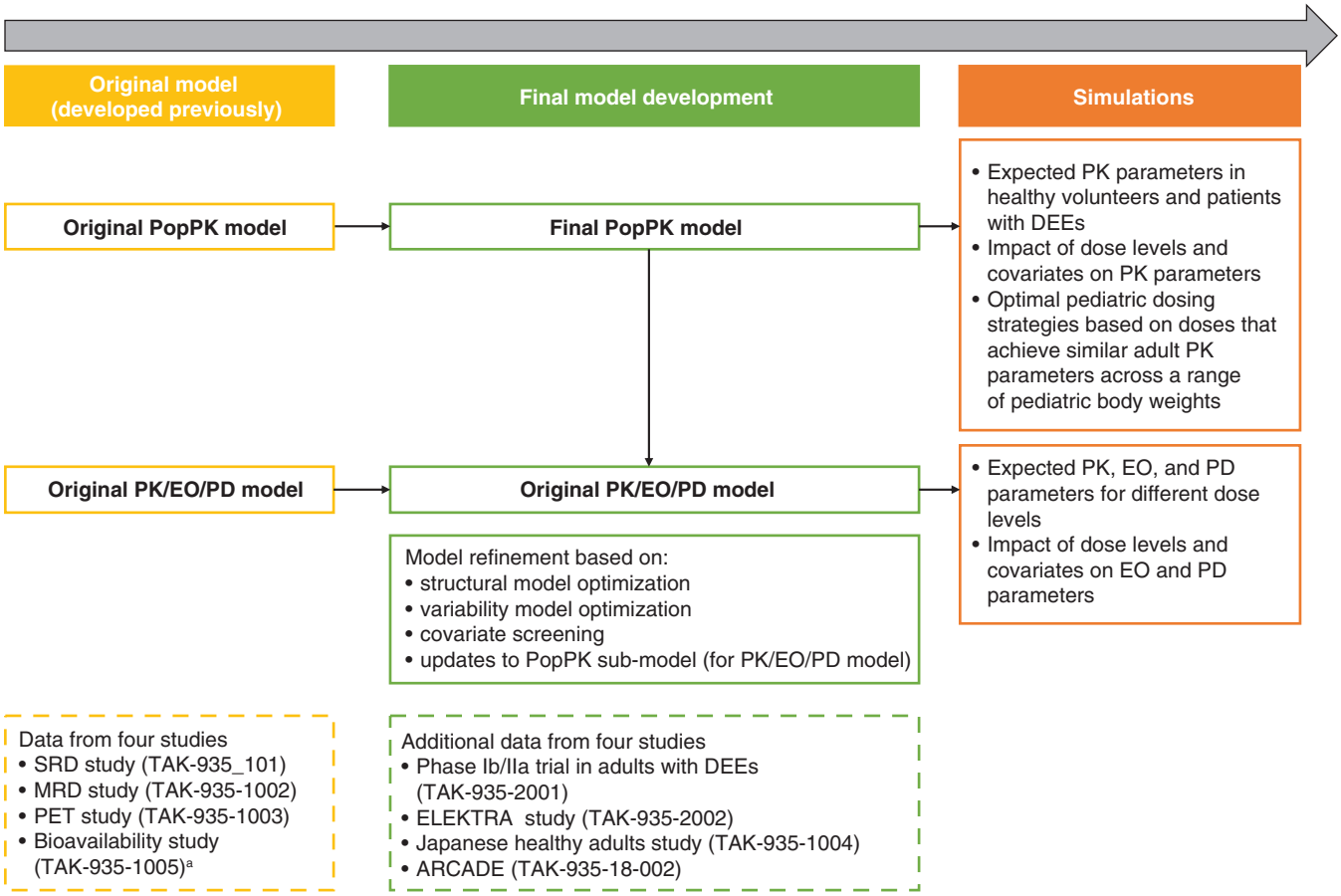

FIGURE 1 Key steps for model development and model-based simulations. Original model development described in Yin et al. (2023).[9] The original PopPK model for soticlestat plasma concentrations in healthy volunteers was refined to reflect the data from patients with DEEs. Subsequently, plasma 24HC concentration data were included in the analysis data set and the final PK/EO/PD model was developed, informed by the final PopPK model and the original PK/EO/PD model, to characterize the PK/PD relationship between soticlestat concentrations and plasma 24HC concentrations. The PK/EO model was not updated because no additional EO data were available. 24HC, 24*S*-hydroxycholesterol; DEE, developmental and epileptic encephalopathy; EO, enzyme occupancy; MRD, multiple-rising dose; PD, pharmacodynamic; PET, positron emission tomography; PK, pharmacokinetic; PopPK, population pharmacokinetic; SRD, single-rising dose.

variability, and objective function values based on the likelihood of the model fit for nested models and Akaike's or Bayesian information criterion for non-nested models.

Base and final models were qualified using prediction-corrected visual predictive checks (with 1000 model-based simulations), which provide a simulation-based method to visually assess concordance of the model-based simulations and observed data. In addition, a standard nonparametric bootstrap with replacement ($n = 1000$) procedure was performed for the final PK/EO/PD model to assess model stability.

Covariate model development and application

Covariate screening was initially performed using F-tests for the reduction in the unexplained variability when adding a covariate on a linear model for individual random effects. Subsequently, a forward inclusion ($p < 0.05$), backward deletion ($p < 0.01$) procedure was applied to determine inclusion in the model. Screened variables were comedications (grouped by PK inducer status: inducer, neutral, or inhibitor), growth and maturation factors (body weight, body mass index [BMI], and age), individual characteristics (ethnic background, epileptic syndrome type, and sex), kidney function factors (creatinine clearance and estimated glomerular filtration rate [eGFR]), liver function factors (alanine aminotransferase, alkaline phosphatase, aspartate aminotransferase, bilirubin, and gamma glutamyl transferase), and protein binding factors (AGP and albumin). Bilirubin and comedications were only screened for inclusion in the PopPK model. The effect of ethnic and regional background was first examined as covariate effects for race (Asian and Black) and then for country (Japanese and Chinese) within the Asian subpopulation, to address inquiries from local regulatory agencies.

Categorical covariates were modeled to derive the percent change between the typical value and the category level of interest.

Continuous covariate effects were scaled using a reference value and tested using a power function. For age, a hockey stick model was also tested to implement age-related changes only up to a given age level.

Model-based simulations were performed to quantify the effects of covariates on PK and PD parameters.

PK and PD parameters were simulated using the PopPK model and PK/EO/PD model, respectively, for a reference patient with characteristics based on the median (for continuous covariates) or most frequent (for categorical covariates) values in the data set, and the effect of different cohort levels was simulated by modifying covariate values one at a time. Simulated PK parameters were area under the plasma concentration–time curve (AUC), maximum plasma drug concentration (C_{max}), and trough plasma concentration (C_{trough}), and simulated PD parameters were steady-state EO and change from baseline 24HC over 12 h at steady-state. Reference patient characteristics were: 200 mg soticlestat b.i.d. dosage, 24-year-old patient of non-Asian ethnic background with a DEE, with body weight 56.6 kg, BMI 21.8 kg/m^2, eGFR 166.2 mL/min/1.73 m^2, and AGP 20 mg/dL. Continuous covariates were simulated at half and twice the reference value, and categorical covariates were simulated at each alternative value.

Simulations

A series of simulations were carried out to identify dosing strategies for use in phase III clinical trials in children with DEEs that would achieve similar exposures and corresponding PD responses to those seen in previous studies with soticlestat.

First, PK, EO, and change from baseline 24HC profiles over time were simulated for 100, 200, and 300 mg b.i.d. soticlestat dosages using the final PK/EO/PD model. The hypothetical treatment schedule was continuous dosing for 21 days followed by a 7-day washout period in a reference patient with a DEE who was aged 45 years, not of Asian descent, and with a body weight of 70 kg.

Second, the final PopPK model was used to simulate various dosing strategies for a range of body weights (10–70 kg) in children aged 2–21 years, with the aim of defining weight-based pediatric dosing recommendations. For each body weight (1 kg steps) and dose strength, 10,000 simulations of steady-state AUC were performed and the percentage of simulations above the reference AUC (based on equivalent adult dosing) were calculated. The reference AUC values for low, medium, and high dosing were 764, 1800, and 3000 ng·h/mL corresponding to values for 100, 200, and 300 b.i.d. dosing in adults, respectively. Recommended doses were derived such that ~35% to 65% of the simulations at the suggested dose had higher AUC values than the respective reference AUC values, respectively.

RESULTS

Study population and demographics

For the PopPK model, data were provided on 218 individuals, of whom 110 (50%) were healthy individuals and 108 (50%) were patients. Mean (standard deviation [SD]) age was 24.1 (14.5) years. For the PK/EO/PD model, data were provided on 306 individuals, of whom 132 (43%) were healthy individuals and 174 (57%) were patients. Mean (SD) age was 21.8 (14.6) years. For both models, 67% of included individuals were of White ethnic background (Table S2).

PopPK model

The final PopPK model consisted of a linear two-compartment model with delayed oral first-order absorption, with random effects for relative bioavailability (F_{rel}), absorption rate constant (k_a), inter-compartmental clearance (Q), and peripheral volume (V_p). A combined additive and proportional error model was used to describe residual variability.

The structural and random effects modeling for the final PopPK model were similar to the original PopPK model. However, the final PopPK model included a covariate for formulation (oral vs. tablet) on absorption lag time and k_a, which was originally implemented using a delay compartment in the original PopPK model.[9] Other included covariate effects in the final PopPK model were: baseline AGP and baseline weight on F_{rel}; dose on k_a, F_{rel}, Q, and V_p; patient status on linear elimination clearance; BMI on k_a (only for participants younger than 18 years); comedication with anti-epileptic drugs grouped as strong CYP3A enzyme inducers (carbamazepine, phenobarbital, and phenytoin) on k_a; eGFR on V_p; Chinese ethnic background (dichotomized as yes or no) on k_a; and ethnic background (categorized as Chinese, Japanese, or non-Asian) on Q. Black as race was not identified as a significant covariate for any of the PK parameters. The effect of body weight on PKs was estimated as covariate effect on F_{rel}. This resulted in a very precise parameter estimate and fit the data significantly

better than fixing the weight effect based on allometric principles. We also kept the estimated weight effects because we did not have other growth-related covariates (e.g., age), which would have correlated with weight and therefore might have interfered with the weight effect parameter estimation.

Table 1a lists the parameter estimates of the final PopPK model. All parameters, except the amount of additional unexplained variability in case of missing AGP concentrations and the k_a, could be estimated with good precision. The main purpose of this model was to characterize the extent of the absorption (AUC), which, based on preclinical data, drives efficacy. Therefore, the low precision of the estimate for the k_a was deemed acceptable. Shrinkage for the random effect parameters was low to moderate (≤30%). The largest shrinkage value was for BSV on Q, which may be due to the lack of information for this parameter. Visual predictive checks and GOF plots indicated that the final model fit the observed data well (Figure 2, Figures S1 and S2). BSV plots for the continuous and categorical variables examined as covariates are shown in Figure S3. NONMEM control streams codes for the final model are provided in the supplementary material (Appendix S1).

Based on simulation analyses with the final PopPK model, steady-state (ss) exposure parameters with 300 mg soticlestat b.i.d. treatment were slightly lower for a patient with a DEE than a healthy volunteer, both with the same reference characteristics (defined in "Section 2"); simulated exposures for the reference patient and reference healthy volunteer, respectively, were 3848 and 2967 ng·h/mL for $AUC_{ss,24}$, 1253 and 1168 ng/mL for $C_{max,ss}$, and 27 and 16 ng/mL for $C_{trough,ss}$. However, differences between healthy volunteers in phase I studies and patients in phase II studies, as well as ethnic differences, are typically multivariate and better assessed by means of summary statistics on the predicted exposure parameters.

The univariate effects of dose and covariates on AUC, C_{max}, and C_{trough} in the final PopPK model are shown as tornado plots in Figure 3; covariate effects were included if there was a change from the reference value of at least 5% based on the simulations (reference characteristics defined in "Section 2").

To address combined effects of multiple covariates, the respective univariate effects would need to be combined or derived using multivariate simulations. For example, Chinese pediatric patients in the ELEKTRA study were predicted to have a 33% higher C_{max} than non-Chinese healthy adult volunteers, based on a multivariate simulation (data not shown). This aligns well with the sum of the three univariate effects: Chinese, patient status, and body weight.

Similar comparison of Japanese participants was not possible because data were only available for healthy adults and not for Japanese patients with DEEs.

PK/EO/PD model

The structural model and random error modeling for the final PK/EO/PD model were unchanged from the original model because no major model misspecifications were identified. The final PK/EO/PD model encompassed a turnover model to characterize changes in 24HC concentrations over time and a maximum inhibition (I_{max}) of 24HC production model for the indirect exposure-effect, with inhibition of 24HC synthesis rates caused by soticlestat exposure. The model also included effect-site concentration (soticlestat exposure in the brain), which was estimated based on plasma soticlestat concentration and implemented as a delayed equilibrium, based on a plasma/brain transit rate parameter estimated in the original model. Random effects were estimated on the baseline 24HC level and half maximal inhibitory concentration. The BSV for major PK and PD parameters was estimated using an exponential error model, except for the I_{max} parameter, when an additive error model was used. During the model development process, 17 out of 2625 observations with conditional weighted residuals over the value of 5 were excluded.

After covariate screening, the final model included baseline AGP, baseline weight, and age (only estimated for those aged under 17.5 years) as covariates on change from baseline 24HC level. The age cutoff was implemented using a hockey stick covariate model. The model also inherited the covariates from the PopPK model that indirectly affected the PD parameters.

Table 1b lists the parameter estimates of the final model. Shrinkage for the random effect parameters was low to moderate, with a maximum value of 20.0%. Visual predictive check and GOF plots showed that the final model fit the observed data well (Figure 2 and Figure S4). BSV plots for continuous and categorical variables examined as covariates are shown in Figure S3. NONMEM control stream codes for the final model are provided in the supplementary material (Appendix S1).

Based on simulation analyses using the final PK/EO/PD model, the effects of covariates and dose on average EO and change from baseline 24HC are shown in Figure 3 for all effects with at least 2.5% change from the reference value (defined in "Section 2") for a patient. Most effects were small, with the largest changes (3.0–7.5% change from reference value) seen with variations in dose from 100 mg to 300 mg. Baseline weight, baseline AGP, and

TABLE 1 Parameter estimates and shrinkage estimates for the PopPK model (a) and PK/EO/PD (24HC) model (b).

(a) PopPK model

Parameter	Role	Estimate	95% CI	Relative SE, %
Absorption rate (k_a)	TV, 1/h	8.39	(−5.68, 22.4)	85.6
	Non-OS formulation effect, %	−43.7	(−125, 37.6)	95.0
	Dose effect, exponent	−0.753	–	Fixed
	BMI effect, exponent	2.24	(2.23, 2.26)	0.3
	Strong CYP3A enzyme inducer effect, %	−66.2	(−87.8, −44.7)	16.6
	Chinese descent effect, %	−63.7	(−94.4, −32.9)	24.6
	BSV[a]	1.02	(0.997, 1.04)	1.2
Elimination clearance (CL)	TV, L/h	4.2	(3.85, 4.54)	4.2
	Patient effect, %	−22.8	(−40.2, −5.51)	38.7
Central volume (V_c)	TV, L	3.01	(2.96, 3.05)	0.8
Distribution clearance (Q)	TV, L/h	1.15	(0.777, 1.53)	16.7
	Dose effect, exponent	−0.218	–	Fixed
	Japanese descent effect, %	−42.7	(−62.1, −23.2)	23.3
	Chinese descent effect, %	−75.7	(−94, −57.4)	12.3
	BSV[a]	0.436	(0.433, 0.439)	0.4
Peripheral volume (V_p)	TV, L	7.8	(7.12, 8.47)	4.4
	Dose effect, exponent	−0.214	–	Fixed
	eGFR effect, exponent	−0.406	(−0.408, −0.404)	0.2
	BSV[a]	0.625	(0.621, 0.629)	0.3
Lag time of the first compartment ($ALAG_1$)	TV, h	0.133	(0.123, 0.142)	3.5
	Non-OS formulation effect, %	23.8	(14.6, 32.9)	19.6
Bioavailability (F_1)	TV	0.0216	–	Fixed
	Dose effect, exponent	0.204	–	Fixed
	Body weight effect, exponent	−0.593	(−0.596, −0.589)	0.3
	AGP effect, exponent	0.544	(0.192, 0.896)	33.0
	BSV explained by AGP, %	0.42	(−2.34, 3.18)	335.6
	BSV[a]	0.527	(0.519, 0.536)	0.8
Residual variability	Proportional, %	48.3	(44.2, 52.5)	4.4
	Additive, ng/mL	0.001	–	Fixed
Shrinkage	SD shrinkage, %			
BSV k_a (eta)	20.9			
BSV Q (eta)	29.9			
BSV V_p (eta)	20.0			
BSV F_1 (eta)	4.0			
Residuals (epsilon)	7.7			

(b) PK/EO/PD (24HC) model

Parameter	Role	Original estimate	Bootstrap			
			Mean	95% CI	Relative SE, %	Bias, %
Baseline 24HC (BL_{24HC})	TV, ng/mL	50.5	50.293	(47.2, 53)	2.9	−0.4
	Age effect cutoff, years	17.5	17.970	(14.9, 23.3)	11.2	2.7
	Age effect, exponent	−0.511	−0.515	(−0.679, −0.37)	15.2	0.7
	AGP effect, exponent	0.215	0.211	(0.0666, 0.347)	34.0	−1.7
	Body weight effect, exponent	−0.256	−0.248	(−0.382, −0.0902)	30.6	−3.2
	BSV[a]	0.0811	0.080	(0.0628, 0.0991)	11.7	−1.6
24HC degradation rate (k_{out})	TV, 1/h	0.0199	0.020	(0.0181, 0.0215)	4.4	−0.3

(Continues)

TABLE 1 (Continued)

(b) PK/EO/PD (24HC) model						
			Bootstrap			
Parameter	**Role**	**Original estimate**	**Mean**	**95% CI**	**Relative SE, %**	**Bias, %**
Maximum inhibition of 24HC production (I_{max})	TV, %	92	91.825	(87.1, 98.1)	3.3	−0.2
Effect-site concentration for 50% maximum effect (IC_{50})	TV, ng/mL	9.85	9.843	(7.26, 13)	15.0	−0.1
	BSV[a]	0.636	0.633	(0.303, 1.06)	30.5	−0.4
Shape parameter (γ)	TV	0.881	0.908	(0.706, 1.17)	13.5	3.1
Residual variability	Additive, ng/mL	3.91	3.913	(3.61, 4.24)	4.1	0.1
Shrinkage	SD shrinkage, %					
BL_{24HC} (eta)	2.3					
IC_{50} (eta)	20.0					
Epsilon	8.5					

Note: Estimates, bootstrap means, and CIs were rounded to three significant digits, relative SE and bias were rounded to one decimal digit.

Abbreviations: 24HC, 24S-hydroxycholesterol; AGP, alpha-1-acid glycoprotein; BMI, body mass index; BSV, between-subject variability; CI, confidence interval; CYP, cytochrome P450; eGFR, estimated glomerular filtration rate; EO, enzyme occupancy; OS, oral solution; PD, pharmacodynamic; PK, pharmacokinetic; PopPK, population pharmacokinetic; SD, standard deviation; SE, standard error; TV, typical value.

[a]Reported on variance scale.

patient status were associated with less than 5% change from the reference value.

Simulations

Simulations using the PK/EO/PD model indicated that with soticlestat 100, 200, and 300 mg b.i.d. for 12 h at steady-state, respectively, average EO (median of individual simulated 24-h average values) was 81.7%, 89.2%, and 92.2%, and average change from baseline 24HC was −71.6%, −80.6%, and −84.1% (Figure 4).

Minimal accumulation for PK and EO parameters based on a hypothetical treatment schedule of 100–300 mg b.i.d. for 21 days followed by a 7-day washout period. Steady-state levels for 24HC inhibition were achieved within a week of treatment and were maintained over time (Figure 4).

Recommended dosing strategies were developed for a study that included participants aged 2–21 years by identifying doses at which ~35% to 65% of the simulations at the doses suggested had higher AUCs than the reference AUC from three adult doses (764, 1800, and 3000 ng·h/mL based on 100, 200, and 300 mg b.i.d. dosing in adults, respectively; Figure 5). Based on these analyses, recommended doses were defined for four pediatric weight bands (10 to <15 kg, 15 to <30 kg, 30 to <45 kg, and 45–100 kg; Table 2).

DISCUSSION

Here, we present the successful application of a modeling strategy to describe the PK and PD profiles of soticlestat in both healthy volunteers and the target patient population of individuals with DEEs. The resulting PopPK and PK/EO/PD models were used to examine how PK and PD profiles are affected by individual characteristics and other covariates that may affect dosing recommendations. The final models were well-fitted to observed PK and PD data from healthy volunteers and patients with DEEs. Furthermore, model-based simulations were used to inform the drug development process for soticlestat by guiding weight-based dosing recommendations for use in phase III clinical trials.

The original PK/EO/PD model developed for healthy volunteers[9] was found to be robust, with minimal changes required to the structural and error-term modeling to extend the PopPK and PK/EO/PD models to apply to patients with DEEs. In support of this, results from two clinical trials of patients with DEEs, in which dosing strategies were informed by the original PK/EO/PD model, indicated that the recommended dosing strategies were appropriate. In both studies, soticlestat treatment led to a numerical reduction in seizure frequency with safety findings that were consistent with previous studies in healthy volunteers.[3,9,10] These

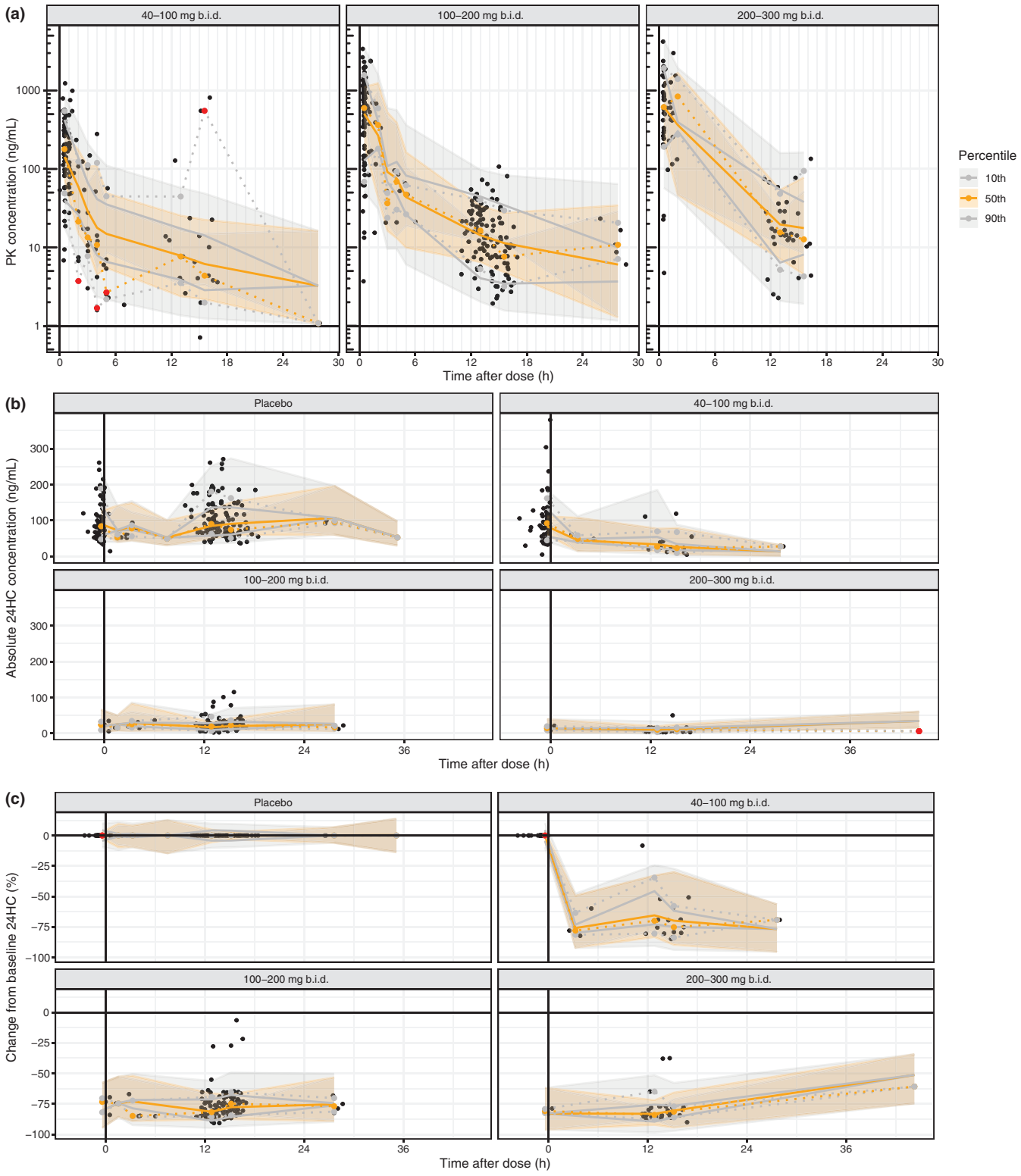

FIGURE 2 Visual predictive checks based on the ELEKTRA study for the final PopPK model (a), for 24HC concentrations based on the final PK/EO/PD model (b), and for 24HC percentage change from baseline based on the final PK/EO/PD model (c). Lines and shaded areas represent median and 95% CI for simulations; dots represent median observations. 24HC, 24*S*-hydroxycholesterol; b.i.d., twice-daily; CI, confidence intervals; EO, enzyme occupancy; PD, pharmacodynamic; PK, pharmacokinetic; PopPK, population pharmacokinetic.

findings support the value of MIDD for optimizing dosing and study design strategies in clinical trials. The present study demonstrates the validity of the original model and describes the extension of the original model with data from patients, which permitted identification of covariates that may impact on dosing decisions and

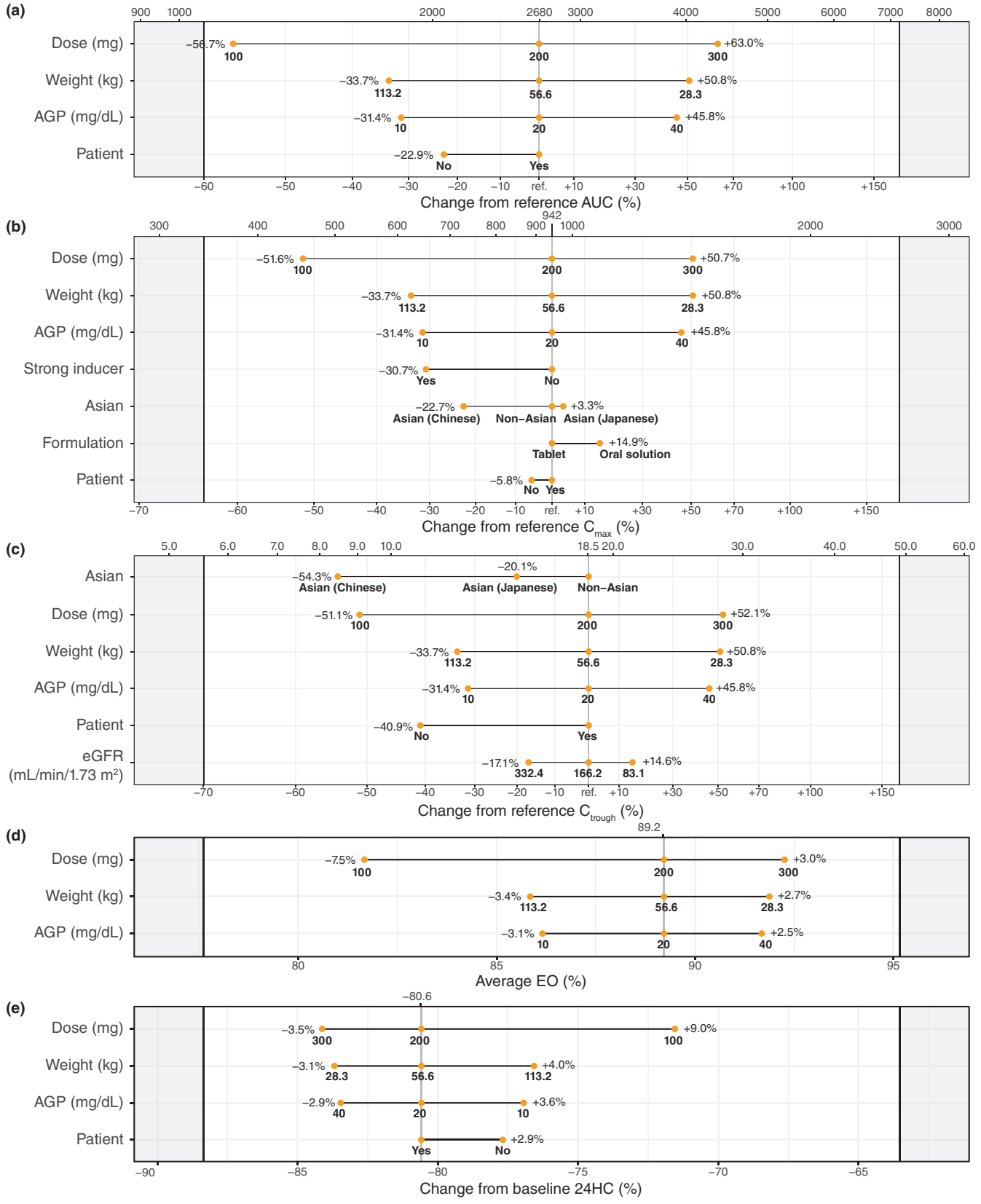

evaluation of potential dosing strategies for phase III trials of soticlestat.

The final PopPK model was a linear two-compartment model with delayed oral first-order absorption. Based on simulations with the final PopPK model, several covariates were found to be associated with soticlestat exposure levels. Changes in body weight and baseline AGP level were associated with the largest changes in soticlestat exposure

FIGURE 3 Tornado plots to illustrate dose and univariate covariate effects on the final PopPK model parameters and on the final PK/EO/PD model parameters; (a) effects on AUC, (b) effects on C_{max}, (c) effects on C_{trough}, (d) effects on EO, and (e) effects on average change from baseline 24HC. Each simulated covariate level is indicated as an orange dot indicating the typical covariate effect on the response variable. The label below each dot illustrates the simulated covariate level and the value above denotes the absolute change from reference. The black vertical lines indicate 80% PI for a reference subject. 24HC, 24S-hydroxycholesterol; AGP, alpha-1-acid glycoprotein; AUC, area under the plasma concentration–time curve; C_{max}, maximum plasma drug concentration; C_{trough}, trough plasma concentration; eGFR, estimated glomerular filtration rate; EO, enzyme occupancy; PD, pharmacodynamic; PI, prediction interval; PK, pharmacokinetic; PopPK, population pharmacokinetic.

out of all the examined covariates. The effect of bodyweight is reflected in the development of weight-based dosing recommendations for children, to ensure that exposure levels are similar to those in adults. Although baseline AGP level was added as a covariate on F_{rel} to account for observed variability, it will not be used for dose adjustment in practice given the high variability of this covariate in response to various factors, including infection. Other identified covariate effects were evaluated in relation to the need for adapted dosing requirements. For example, compared with patients of non-Asian background, patients of Chinese descent were predicted to have a lower C_{max} and lower C_{trough}, and patients of Japanese descent were predicted to have a lower C_{trough}. Because patients of Chinese or Japanese descent were predicted to have similar profiles to patients of other ethnic backgrounds for AUC, average EO, and change from baseline 24HC, dose adjustment for these patient populations was not considered to be necessary.

The use of strong CYP3A inducers alongside soticlestat and receiving soticlestat in a tablet formulation were both associated with a reduced C_{max}. In clinical settings, use of soticlestat alongside ASMs that are strong CYP3A inducers is not expected to be a cause for clinical concern because no effects of strong CYP3A inducers were seen for other PK or PD parameters. Additionally, the covariate screening did not identify an impact for any other ASMs on soticlestat PK and PD profiles. In terms of dose itself, AUC was shown to increase in a slightly greater than dose-proportional manner, whereas C_{max} and C_{trough} increased in a dose-proportional manner within the range of soticlestat 100–300 mg b.i.d.

The final PK/PD model was an indirect link turnover model with an inhibitory effect of exposure on the 24HC production rate. Based on the final model, average EO during one dosing interval at steady-state was predicted to be 81–92% for 100–300 mg b.i.d. treatment. Average change from baseline 24HC during one dosing interval at steady-state was predicted to be ~71–81% after 100–300 mg b.i.d. treatment. Identified covariates had minor effects on the average EO and change from baseline 24HC. Further simulations indicated that soticlestat concentration and EO steady-states were almost instantaneously reached. A well maintained steady-state level for 24HC inhibition was achieved within a week of treatment and, after stopping treatment, 24HC levels were simulated to return to baseline within 7 days.

Based on simulations with the final PK/EO/PD model, recommended dosing strategies were developed for four pediatric weight bands. These findings highlight the utility of PK/EO/PD modeling and MIDD to expedite the development of therapies for rare conditions, such as DS and LGS, and is substantiated by the use of MIDD in other drug development scenarios.[3,10,13] As shown in the present study, clinical trial simulations allow quantification of uncertainty about dose selection and the effect of covariates, which can help to determine the required sample size and appropriate dosing strategies.[14] This is particularly important in conditions affecting children, given the differences between adults and children in body composition, physiology, and biochemistry that may alter dosing requirements.[13]

To address the urgent unmet needs of the DS and LGS patient population, we used a "learn-confirm-translate" approach, linking PK and PD with safety and efficacy. Initially, we assessed the safety and PK/PD/EO in healthy volunteers, focusing on changes in 24HC levels and EO as our primary PD measures. Nonclinical animal model studies helped to establish the required extent of EO for maximal efficacy. Together, these findings guided our study design for clinical trials in patients, beginning with adults with DEEs. We then leveraged insights from healthy volunteers and adult patients to ascertain appropriate dosing regimens for pediatric patients with DS and LGS.

This process of development involved careful exposure matching to determine pediatric dosages, which were then validated in clinical trials. By using pharmacostatistical methods and evaluating the translatability of biomarker responses alongside safety data, we were able to accelerate the development of soticlestat for the pediatric patient population, ensuring their unmet treatment need was addressed as quickly as possible.

Strengths of this study include the breadth of data and populations included in the model. Inclusion of healthy volunteers and patients, children and adults, and participants with various ethnic backgrounds led to a large sample size and allowed the effect of various covariates to be

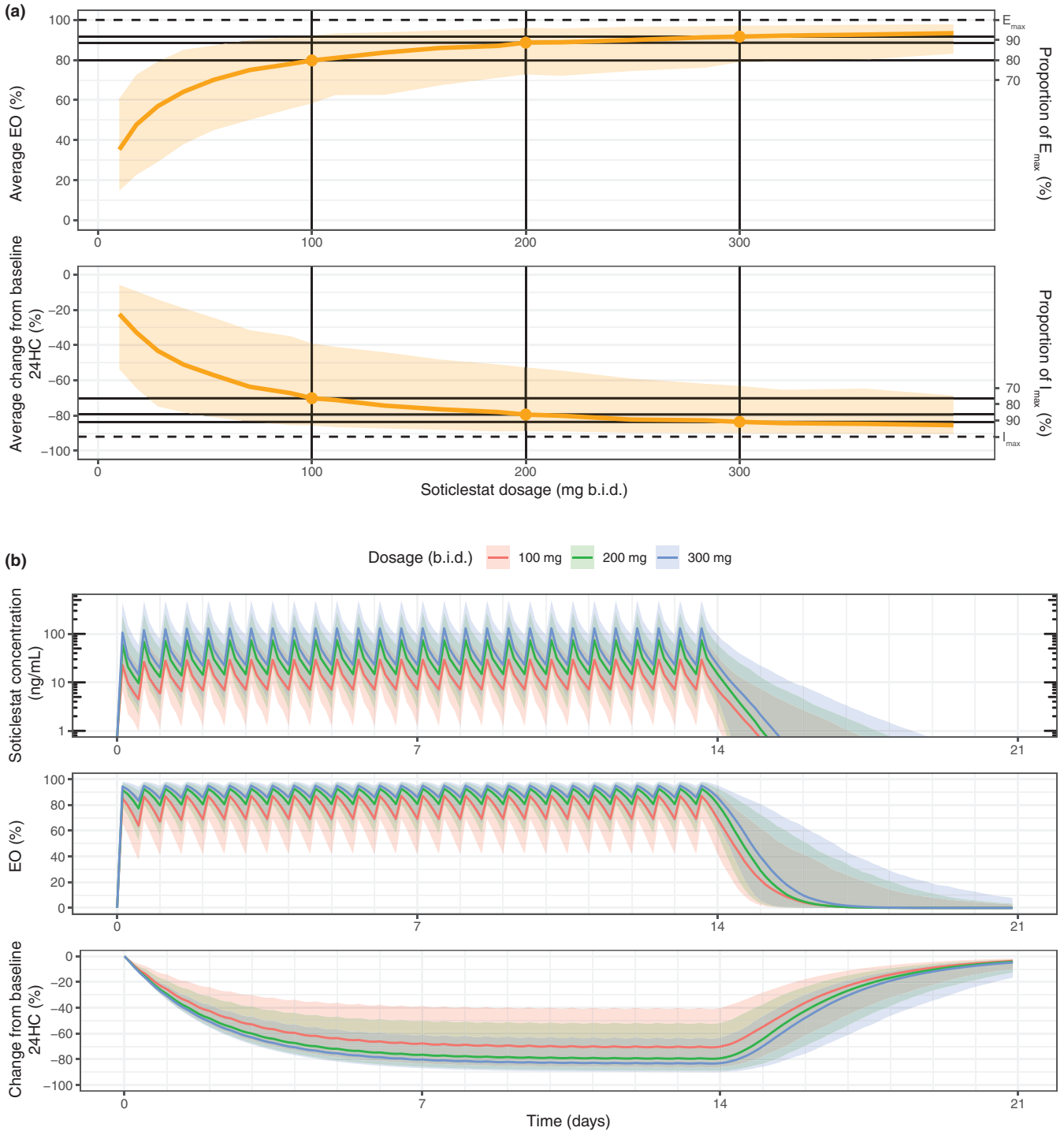

FIGURE 4 Simulations of the dose–response relationship for average EO and percent change from baseline 24HC during 12 h at steady-state (a) and of soticlestat concentrations, EO, and percent change from baseline 24HC over time (b). Simulations were performed with BSV and summarized as median (solid line) and 90% PIs (shaded area). In panel (a), the left y-axis for the EO plots shows the results as percent of the maximum occupancy (E_{max} = 100%, dashed reference line) and for the change from baseline 24HC plots, it shows percent from maximum inhibition (I_{max} = −92%, dashed reference line). 24HC, 24S-hydroxycholesterol; b.i.d., twice-daily; BSV, between-subject variability; E_{max}, maximum EO; EO, enzyme occupancy; I_{max}, maximum inhibition of 24HC production; PI, prediction interval.

evaluated in the models. Additionally, model-based simulations were successfully used to develop pediatric dose recommendations for use in phase III clinical trials along with consideration of other dosing strategy factors, such as ease of administration by caregivers. This MIDD approach to dose selection highlights the potential to expedite drug development by using a data-driven approach to identify dosing strategies that achieve target PK, EO, and

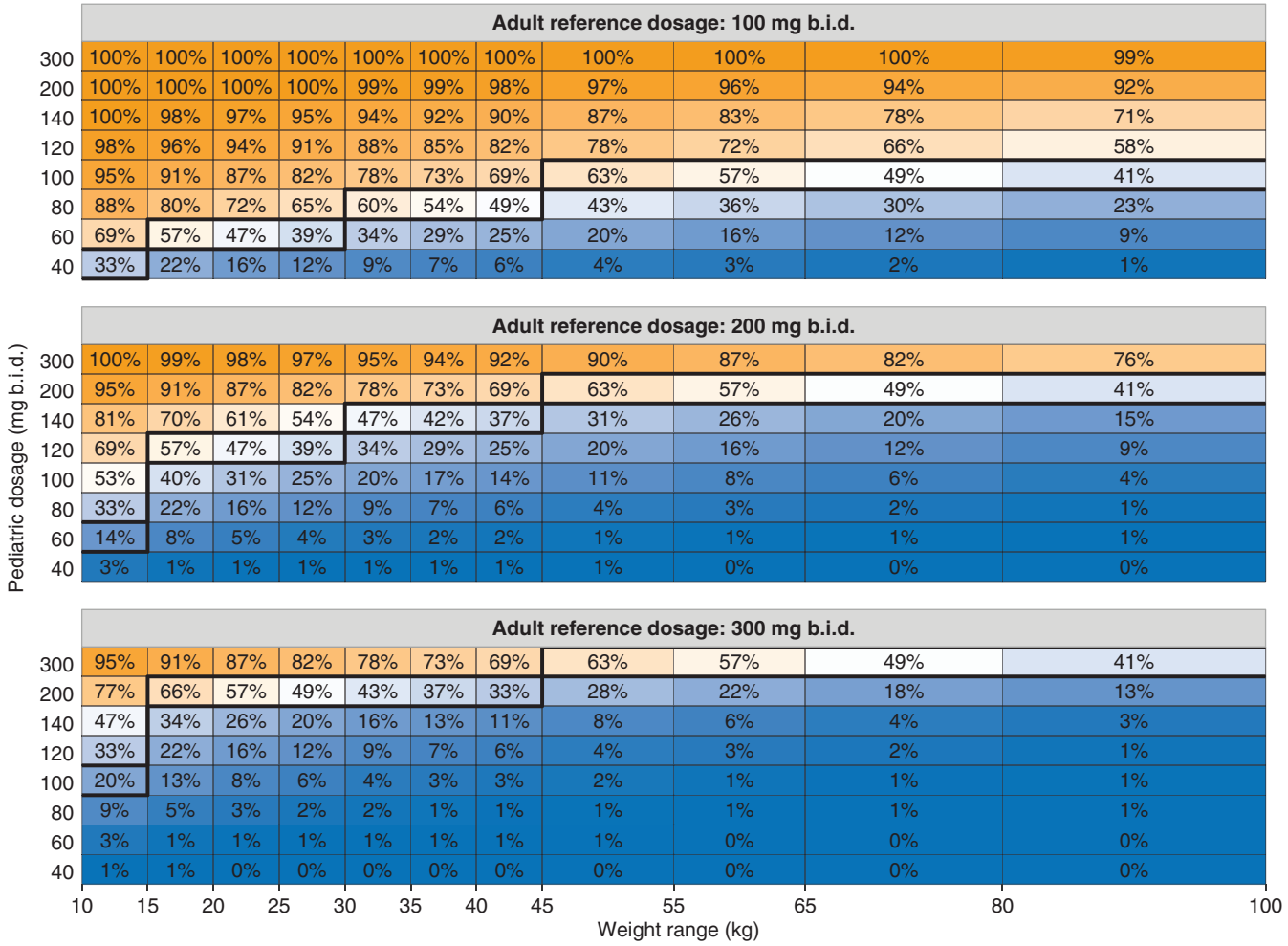

FIGURE 5 Percentage of simulated AUC values greater than the reference adult AUC values at different pediatric weights and dosages. The figures are color-coded and include a contour line, indicating the pediatric dosage (per kg body weight) not exceeding the reference AUC values in ~35% to 65% of all simulated children. AUC, area under the plasma concentration–time curve; b.i.d., twice-daily.

TABLE 2 Pediatric dosing recommendations based on simulations.

Pediatric weight range	Adult reference		
	100 mg b.i.d.	**200 mg b.i.d.**	**300 mg b.i.d.**
≥10 to <15 kg	40 mg b.i.d. 32.9% 818 (339, 1960)	60 mg b.i.d. 13.9% 1330 (553, 3190)	100 mg b.i.d. 19.5% 2460 (1020, 5910)
≥15 to <30 kg	60 mg b.i.d. 47.3% 995 (409, 2410)	120 mg b.i.d. 47.3% 2290 (942, 5550)	200 mg b.i.d. 56.9% 4240 (1740, 10,300)
≥30 to <45 kg	80 mg b.i.d. 53.8% 1080 (449, 2590)	140 mg b.i.d. 41.4% 2120 (880, 5090)	200 mg b.i.d. 37.1% 3260 (1350, 7820)
≥45 to ≤100 kg	100 mg b.i.d. 49.6% 1030 (420, 2500)	200 mg b.i.d. 49.6% 2360 (968, 5760)	300 mg b.i.d. 49.6% 3850 (1580, 9380)

Note: Median (90% PI) AUC in h.ng/mL for adult reference dosages were 1030 (432, 2470), 2380 (995, 5700), and 3870 (1620, 9280) for the 100 mg b.i.d., 200 mg b.i.d., and 300 mg b.i.d. dosages, respectively.

The top line of each cell provides the selected pediatric dosage, the second line provides the probability that individual pediatric AUC_{24} levels exceed the adult reference median AUC_{24}, and the third line provides the median (90% PI) ng·h/mL.

Abbreviations: AUC_{24}, area under the plasma concentration–time curve from 0 to 24 h; b.i.d., twice-daily; PI, prediction intervals.

PD profiles and are therefore expected to optimize efficacy and safety outcomes in the target population.

A key limitation of the study is that soticlestat exhibits complex absorption characteristics, which were only approximately characterized by the model because the focus was on the extent of absorption (AUC). Additionally, sparse samples in the patient population limited a full characterization of the absorption phase. The multiple modes of drug delivery that were used to help with treatment adherence (e.g., crushed vs. non-crushed tablets and via gastrostomy tube) also probably contributed to data variability.

In conclusion, the final model accurately described the PK, EO, and PD characteristics of soticlestat in healthy volunteers and patients with DEEs. Covariate analysis and model-based simulations were able to provide valuable information to guide dosing strategies in phase III clinical trials of soticlestat in patients with DS or LGS.

AUTHOR CONTRIBUTIONS

W.Y., A.F., M.A., G.L., and M.V. wrote the manuscript, designed the research, and performed the research; W.Y., A.F., G.L., and M.V. analyzed the data.

ACKNOWLEDGMENTS

All studies were funded by the sponsor, Takeda Pharmaceutical Company Ltd. Under the direction of the authors and funded by Takeda Pharmaceutical Company Ltd, Emma Butcher, PhD, and Aimee Jones, DPhil (https://orcid.org/0000-0003-0279-1814), of Oxford PharmaGenesis, Oxford, UK, provided writing assistance for this publication, in compliance with current Good Publication Practice guidelines. Editorial assistance in formatting, proofreading, copyediting, and fact-checking was also provided by Oxford PharmaGenesis. The content of this manuscript, the interpretation of the data, and the decision to submit the manuscript for publication in *Clinical and Translational Science* were made by the authors independently.

FUNDING INFORMATION

All studies included in this manuscript were funded by the sponsor, Takeda Pharmaceutical Company Ltd.

CONFLICT OF INTEREST STATEMENT

W. Yin and M. Asgharnejad are employees of Takeda Pharmaceutical Company Ltd and own stock or stock options. M. Vakilynejad is a former employee of Takeda Pharmaceutical Company Ltd. A. Facius and G. Lahu are former employees of Takeda and received payment for acting as consultants for Takeda at the time of data analysis.

DATA AVAILABILITY STATEMENT

The data sets, including the redacted study protocol, redacted statistical analysis plan, and individual participants data of the completed studies supporting the results reported in this article, will be available 3 months after the submission of a request, to researchers who provide a methodologically sound proposal. The data will be provided after its de-identification, in compliance with applicable privacy laws, data protection, and requirements for consent and anonymization.

ORCID

Wei Yin https://orcid.org/0000-0002-4834-5783
Mahnaz Asgharnejad https://orcid.org/0000-0001-8060-2148

REFERENCES

1. Hebbar M, Mefford HC. Recent advances in epilepsy genomics and genetic testing. *F1000Res*. 2020;9:185. doi:10.12688/f1000research.21366.1
2. Johannessen Landmark C, Potschka H, Auvin S, et al. The role of new medical treatments for the management of developmental and epileptic encephalopathies: novel concepts and results. *Epilepsia*. 2021;62:857-873. doi:10.1111/epi.16849
3. Halford JJ, Sperling MR, Arkilo D, et al. A phase 1b/2a study of soticlestat as adjunctive therapy in participants with developmental and/or epileptic encephalopathies. *Epilepsy Res.* 2021;174:106646. doi:10.1016/j.eplepsyres.2021.106646
4. Nishi T, Kondo S, Miyamoto M, et al. Soticlestat, a novel cholesterol 24-hydroxylase inhibitor shows a therapeutic potential for neural hyperexcitation in mice. *Sci. Rep.* 2020;10:17081. doi:10.1038/s41598-020-74036-6
5. Paul SM, Doherty JJ, Robichaud AJ, et al. The major brain cholesterol metabolite 24(S)-hydroxycholesterol is a potent allosteric modulator of N-methyl-D-aspartate receptors. *J. Neurosci.* 2013;33:17290-17300. doi:10.1523/JNEUROSCI.2619-13.2013
6. Nury T, Zarrouk A, Mackrill JJ, et al. Induction of oxiapoptophagy on 158N murine oligodendrocytes treated by 7-ketocholesterol-, 7beta-hydroxycholesterol-, or 24(S)-hydroxycholesterol: protective effects of alpha-tocopherol and docosahexaenoic acid (DHA; C22:6 n-3). *Steroids*. 2015;99:194-203. doi:10.1016/j.steroids.2015.02.003
7. La DS, Salituro FG, Martinez Botella G, et al. Neuroactive steroid N-methyl-d-aspartate receptor positive allosteric modulators: synthesis, SAR, and pharmacological activity. *J. Med. Chem.* 2019;62:7526-7542. doi:10.1021/acs.jmedchem.9b00591
8. Petrov AM, Pikuleva IA. Cholesterol 24-hydroxylation by CYP46A1: benefits of modulation for brain diseases. *Neurotherapeutics*. 2019;16:635-648. doi:10.1007/s13311-019-00731-6
9. Yin W, Facius A, Wagner T, et al. Population pharmacokinetics, enzyme occupancy, and 24S-hydroxycholesterol modeling of soticlestat, a novel cholesterol 24-hydroxylase inhibitor, in healthy adults. *Clin. Transl. Sci.* 2023;16:1149-1162. doi:10.1111/cts.13517
10. Hahn CD, Jiang Y, Villanueva V, et al. A phase 2, randomized, double-blind, placebo-controlled study to evaluate the efficacy and safety of soticlestat as adjunctive therapy in pediatric patients with Dravet syndrome or Lennox-Gastaut syndrome (ELEKTRA). *Epilepsia*. 2022;63:2671-2683. doi:10.1111/epi.17367

11. Takeda. A study to evaluate the safety, tolerability and pharmacokinetics of single ascending dose and multiple doses with titration of TAK-935 in healthy Japanese participants. Accessed November 22, 2023. https://clinicaltrials.gov/ct2/show/NCT04461483
12. Demarest S, Jeste S, Agarwal N, et al. Efficacy, safety, and tolerability of soticlestat as adjunctive therapy for the treatment of seizures in patients with Dup15q syndrome or CDKL5 deficiency disorder in an open-label signal-finding phase II study (ARCADE). *Epilepsy Behav.* 2023;142:109173. doi:10.1016/j.yebeh.2023.109173
13. Bi Y, Liu J, Li F, et al. Model-informed drug development in pediatric dose selection. *J. Clin. Pharmacol.* 2021;61(Suppl 1):S60-S69. doi:10.1002/jcph.1848
14. Bedding A, Scott G, Brayshaw LL, et al. *Clinical trial simulations – an essential tool in drug development*. Bringing Medicines to Life (Abpi); 2013.

SUPPORTING INFORMATION

Additional supporting information can be found online in the Supporting Information section at the end of this article.

How to cite this article: Yin W, Facius A, Asgharnejad M, Lahu G, Vakilynejad M. Population pharmacokinetics, enzyme occupancy, and pharmacodynamic modeling of soticlestat in patients with developmental and epileptic encephalopathies. *Clin Transl Sci*. 2024;17:e13722. doi:10.1111/cts.13722